Draft version August 13, 2014
Preprint typeset using LaTeX style emulateapj v. 5/2/11

arXiv:1408.2702v1 [astro-ph.GA] 12 Aug 2014

Maximum likelihood fits to a cored halo enclosing finite mass

K. A. S. Croker
Department of Physics and Astronomy, University of Hawai'i at Mānoa, Honolulu, HI 96822
Draft version August 13, 2014

ABSTRACT

The hybrid Ricci scalar $R_{\mu\nu}\eta^{\mu\nu}$ formed from a Robertson-Walker derived Ricci tensor and a distinct flat space metric becomes a dark, pseudo-isothermal density under asymptotic constraint. While extension of this constraint to more general scenarios is unclear, it is model independent and suggestive of a radical premise: all galactic dark matter halos are sourced by very many distinct Robertson-Walker spacetimes. We explore this premise and present a cored galactic halo, which encloses finite mass over all space. We compute fit parameters to published data on the Milky Way dwarf spheroidal galaxies, and find consistency with a predicted reciprocal square scaling relation. Spherical symmetry permits treatment of each individual halo as a point particle interacting under a modified gravitational force. This force is Newtonian at large separation with a leading dipole correction, and naturally softens to zero at small separation. Taken as cold dark matter, ensembles of such halos present a possible resolution to tension between large-scale N-body simulations and small-scale astrophysical data.

Subject headings: phenomenology, dark matter, galactic halo

1. INTRODUCTION

Galactic dynamics provided the first evidence (Zwicky 1937) that dominant mass contributions to structure on 100pc-10kpc scales are non-luminous. Contemporary cosmological investigations (Hinshaw et al. 2013; Ade et al. 2013) have also unambiguously demonstrated the dominant fraction of all matter in the universe is non-luminous. Leading candidates for this missing matter (Bertone et al. 2005) are any of a plethora of beyond-the-standard-model particles, those weakly interacting being favoured for their relic behaviour in the early universe and their direct detection possibilities. Further, particulate N-body simulations (Springel et al. 2005) have shown good qualitative agreement with the observed large scale structure (Ahn et al. 2012). Yet, predictions from N-body simulation of particulate cold dark matter (CDM) on galactic scales has remained in significant tension (de Blok 2010) with small-scale astrophysical data. In particular, recognition that the classical Milky Way dwarf-spheroidal galaxies (dSphs) provide excellent test-beds for dark matter dominated stellar systems (Mateo 1998), has provided strong evidence (Walker & Peñarrubia 2011) that the radially divergent "cuspy" halos favoured by N-body CDM simulations are far less likely than asymptotically similar but "cored" halos that approach a constant density as $r \to 0$. Further, this tension persists even in scenarios that consider self-interacting dark matter (Zavala et al. 2013).

While traditional dark matter profiles have been phenomenological (Begeman et al. 1991; Burkert 1995; Navarro et al. 1997), an unexpected result concerning dark matter has emerged from asymptotic constraint of a purely *geometric* quantity. In particular, it can be shown that the vanishing at spatial infinity of a hybrid Ricci scalar $R_{\mu\nu}\eta^{\mu\nu}$, formed from a flat-space metric and the Ricci tensor derived from a distinct Robertson-Walker (RW) metric, not only induces inflationary dynamics within the RW metric, but becomes a contribution which, if interpreted as an energy density within the flat-space, gives a dark, pseudo-isothermal sphere (PITS) density that eventually damps in time. While this result has unrealistic quantitative behaviour, it is model independent and suggestive of a radical premise: perhaps *all* galactic dark matter halos are a consequence of *very many* distinct RW spacetimes. In such a scenario, the smallest unit of CDM is no longer a mass point, but the galactic halo itself.

In the following, we will explore this premise and produce a cored halo profile asymptotic to $1/r^4$. We will exhibit experimental consistency of this new profile with the dSphs and show how such a halo can be modeled as a single dark matter particle interacting with other halos and baryons through distinct gravitational force laws. We will argue that since the force laws are Newtonian at large separation, but diminish linearly to zero at small separation, these halos may ease tension between known agreement of CDM N-body simulation at large scales and astrophysical observation at small scales. Finally, we will consider limitations of our construction and briefly summarize the work presented. Units throughout will be such that $G \equiv c \equiv 1$ unless otherwise indicated.

2. HALO CONSTRUCTION

Given a flat metric

$$\eta_{\mu\nu} = -\mathrm{d}t^2 + \mathrm{d}r^2 + r^2\mathrm{d}\Omega^2 \tag{1}$$

and a distinct Robertson-Walker (RW) metric

$$g_{\mu\nu} = -\mathrm{d}t^2 + a^2(t)\left(\frac{\mathrm{d}r^2}{1+|\kappa_A|r^2} + r^2\mathrm{d}\Omega^2\right) \tag{2}$$

with spatial curvature $\kappa_A < 0$ and scale factor $a(t)$ defined on a common manifold, it can be shown that the constraint

$$\lim_{r\to\infty} R_{\mu\nu}\eta^{\mu\nu} \equiv 0 \tag{3}$$

kcroker@phys.hawaii.edu

not only induces inflationary dynamics within the RW spacetime, but produces a PITS dark halo

$$\rho_h \equiv R_{\mu\nu}\eta^{\mu\nu} \propto \frac{1}{(3+2a^2)^3}\frac{|\kappa_A|}{1+|\kappa_A|r^2} \tag{4}$$

with $a \sim t\sqrt{|\kappa_A|}$. In effect, the constraint (3) preferentially selects the radial pressure term R_{rr} from the RW Ricci tensor. For a self-contained derivation of this result, we refer the reader to the Appendix.

In contrast to phenomenological PITS profiles where core radius r_0 and central density ρ_0 are free parameters, $|\kappa_A|$ interestingly sets both the density *and* distance scale. Yet the density (4) damps in time, and therefore cannot viably seed structure formation. Further, a PITS profile is physically untenable as it encloses divergent mass over all space.

2.1. *A conformally flat RW halo*

To construct an improved halo, consider the conformally flat RW metric

$$g_{\mu\nu} = -\mathrm{d}t^2 + \frac{16a^2(t)}{(4+\kappa_A l^2)^2}\left(\mathrm{d}l^2 + l^2\mathrm{d}\Omega^2\right) \tag{5}$$

with radial spacelike coordinate l, scale factor a, and spatial curvature $\kappa_A \neq 0$. The Ricci tensor for (5) is

$$R_{ll} = 16\frac{2\kappa_A + a\ddot{a} + 2\dot{a}^2}{(4+\kappa_A l^2)^2} \qquad R_{tt} = -\frac{3\ddot{a}}{a} \tag{6}$$
$$R_{\theta\theta} = R_{ll}l^2 \qquad R_{\phi\phi} = R_{ll}l^2\sin^2\theta.$$

where dots denote derivatives with respect to coordinate time. Note that R_{ll} with $\kappa_A > 0$ takes the form of a cored halo density, with the desirable property that it would enclose finite mass over all space. This can be seen because $|R_{ll}| \sim 1/l^4$ and so the enclosed mass integral

$$4\pi\int_0^\infty R_{ll}l^2\ dl < \infty. \tag{7}$$

is finite. Unfortunately, in the conformally flat representation (5), constraint (3) is trivial as all but R_{tt} vanish as $l \to \infty$.

2.2. *Phenomenological assumption*

To proceed, recall that the temporal damping of expression (4) is consequence of $a(t) \propto t$: the RW scale factor grows linearly and thus describes an unrealistic vacuum Milne universe. Suppose that, in the presence of matter fields influencing the RW spacetime, the constraint (3) is no longer appropriate, but that a more appropriate constraint continues to preferentially select a radial pressure contribution from the Ricci tensor. We do not speculate on the precise form of this constraint, only its existence. This qualitative behaviour suggests the following dark contribution

$$\rho_h = R_{rr}\eta^{rr} \propto 16\frac{a\ddot{a} + 2\dot{a}^2 + \kappa_A}{(4+\kappa_A l^2)^2} \tag{8}$$

where we have made the naive identification $r = l$.

Having established desirable spatial behaviour, we proceed with a Copernican Principle and consider RW matter fields reasonably like our own: a matter-dominated scale factor

$$a(t) = (t\sqrt{6\pi\rho_A})^{2/3} \tag{9}$$

with some present day matter density ρ_A. Substitution of equation (9) into the numerator of equation (8) gives the following temporal behaviour

$$\rho_h \propto \left[\kappa_A + \frac{2}{3}\left(\frac{6\pi\rho_A}{t}\right)^{2/3}\right]. \tag{10}$$

If $\kappa_A < 0$, apart from overall sign, this temporal behaviour is reminiscent of accretion and implies a density that starts from zero at some time in the past and grows monotonically to

$$\lim_{t\to\infty}\rho_h = -\frac{16|\epsilon||\kappa_A|}{\pi\left(4-|\kappa_A|r^2\right)^2} \tag{11}$$

where we have explicitly introduced a proportionality constant $\epsilon/\pi < 0$. Given appropriate choice of ρ_A, this temporal behavior could plausibly seed structure but expression (11) spuriously diverges to infinity at $r = 2/\sqrt{\kappa_A}$.

In the presence of N metrics, it is well-known (Boulanger et al. 2001) that the only consistent linearized gravity theory is N distinct statements of General Relativity. It is thus reasonable to assume that our RW spacetime and our flat spacetime both satisfy their own, separate, Einstein equations. Each Einstein equation, however, exhibits the familiar four-fold coordinate freedom so there is no *a priori* need to demand an identity relation between the coordinates of metric (1) and those of metric (5). If we instead introduce the following relation

$$l \equiv ir \implies \mathrm{d}l = i\mathrm{d}r. \tag{12}$$

then the large t limit of expression (8) becomes

$$\lim_{t\to\infty}\rho_h = \frac{16|\epsilon||\kappa_A|}{\pi\left(4+|\kappa_A|r^2\right)^2}. \tag{13}$$

This is a cored density, consistent with astrophysical observation on galactic scales, and encloses a finite mass

$$M_A = \frac{2^3|\epsilon|\pi}{\sqrt{|\kappa_A|}} \tag{14}$$

over all space. Henceforth, we will drop the absolute value signs on ϵ and refer to these halos as Boulanger Astrophysically Motivated (BAM) halos.

In summary, we have assumed the existence of a generalized constraint which, analogous to equation (3), preferentially selects the radial pressure term of a distinct Ricci tensor. This tensor is sourced by a distinct RW spacetime coupled to its own matter fields through an Einstein equation. This construction leads to a phenomenological halo profile (13) with novel properties which we now explore.

2.3. *Observational consistency of BAM halos*

Regarding the density (13) as a matter source within the flat spacetime, Newtonian superposition allows one to introduce an arbitrary number of BAM halos. Given Cartesian locations

$$P \equiv \{(x_i, y_i, z_i)\}_{i=0}^N \tag{15}$$

TABLE 1
BAM halo fit parameters for the classical Milky Way dwarf spheroidal galaxies

Object	$\log_{10}\left[\rho_0/M_\odot \mathrm{pc}^{-3}\right]$	$\log_{10}\left[r_0/\mathrm{pc}\right]$
Car	$-0.20^{+0.14}_{-0.16}$	$2.59^{+0.19}_{-0.12}$
Dra	$0.13^{+0.12}_{-0.12}$	$2.71^{+0.13}_{-0.15}$
For	$-0.46^{+0.03}_{-0.05}$	$2.84^{+0.03}_{-0.02}$
Leo I	$0.20^{+0.12}_{-0.14}$	$2.55^{+0.16}_{-0.10}$
Leo II	$0.36^{+0.18}_{-0.24}$	$2.38^{+0.24}_{-0.13}$
Scl	$0.19^{+0.09}_{-0.11}$	$2.49^{+0.07}_{-0.06}$
Sex	$-0.47^{+0.22}_{-0.56}$	$2.87^{+0.18}_{-0.26}$
UMi	$0.10^{+0.10}_{-0.16}$	$2.57^{+0.18}_{-0.09}$

FIG. 1.— Graph of Table 1 (black, solid squares). The line (dashed, blue) gives a least squares fit determined from averaged asymmetric uncertainties along both axes, excluding the tidally stripped dSph Draco (green, hollow square).

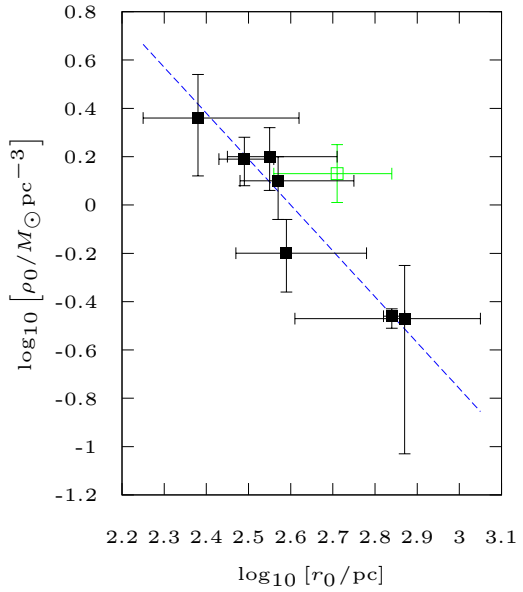

within the flat spacetime, one may perform the above construction with N distinct RW spacetimes, associating each spacetime's radial coordinate origin with some $p \in P$.

To facilitate investigation of the proposed density (13), it is convenient to define parameters analogous to central density ρ_0 and core radius r_0 of more familiar phenomenological profiles

$$\rho_0 \equiv \frac{\epsilon|\kappa_A|}{\pi} \qquad r_0 \equiv \frac{1}{\sqrt{|\kappa_A|}}. \tag{16}$$

Note that the algebraic dependence between ρ_0 and r_0 in equations (16) implies the testable relation

$$\log_{10}\rho_0 = -2\log_{10} r_0 + \log_{10}\frac{\epsilon}{\pi}. \tag{17}$$

To investigate this prediction, we have computed the BAM fit parameters ρ_0 and r_0 for the dSphs. These data are presented in Table 1. Errors enclose the central 68% of area under the marginalized 1D probability distribution function, determined via Monte Carlo analysis of velocity dispersion data fit to a Jeans model for the visible mass motion, assuming a Plummer luminous distribution. For analysis details, see Walker et al. (2009, 2010); Salucci et al. (2012). A least squares fit gives the following slope and intercept

$$\frac{\mathrm{d}\log_{10}\rho_0}{\mathrm{d}\log_{10} r_0} = -2.01 \pm 0.39 \tag{18}$$

$$\log_{10}\frac{\epsilon}{\pi} = 5.26 \pm 1.10 \tag{19}$$

consistent with our prediction of -2. Noting the uncertainties in values (18) and (19) are rather large, we recall that Draco is very likely tidally stripped. Indeed, dropping Draco from the fit gives

$$\frac{\mathrm{d}\log_{10}\rho_0}{\mathrm{d}\log_{10} r_0} = -1.90 \pm 0.13 \tag{20}$$

$$\log_{10}\frac{\epsilon}{\pi} = 4.94 \pm 0.37 \tag{21}$$

again consistent with our prediction of -2, with uncertainties now less than 10% in both parameters. Proceeding without Draco, from the intercept, one may compute the dimensionless proportionality constant

$$\epsilon = (1.31 \pm 0.48) \times 10^{-8}. \tag{22}$$

One might object that the slope (20) is in tension with an existing (Salucci et al. 2012; Donato et al. 2009) scaling relation $\rho_0 \propto r_0^{-1}$ between Burkert profile halo parameters for the dSphs. While it has been argued elsewhere (Donato et al. 2009) that a constant $\log \rho_0 r_0$ hypothesis is insensitive to the specific cored profile assumed, the displayed (Salucci et al. 2012; Donato et al. 2009) agreement is not as pronounced for the dSphs as for the other objects surveyed. Considering the particularly clean probe of dark distribution capable within the dSphs, and that our BAM fit parameters are obtained via the identical method and data as Salucci et al. (2012), the extreme low end of the galaxy mass scale may warrant renewed attention.

3. BAM HALO AS POINT-LIKE CDM

Spherical symmetry of the BAM density (13) permits treatment of halo-baryon and halo-halo gravitational interactions as pointlike two-body interactions, with an altered gravitational force law. Consider two distinct BAM halos with curvature parameters κ_A and κ_D. We now calculate the halo-baryon interaction potential $\Phi_{hb}(z)$ and the halo-halo interaction potential $\Phi_{hh}(z)$. It should be emphasized that the usual gravitational interaction for baryon-baryon interactions is unchanged.

3.1. *Halo-baryon interaction*

By spherical symmetry, the halo-baryon interaction is readily found via the Gauss law

$$\mathbf{F}(z) = -\frac{M_{\mathrm{H}}(z) m_b}{z^2}\hat{\mathbf{z}} \tag{23}$$

where m_b is the mass of the baryon, z is the physical separation between the baryon and the mass center of

FIG. 2.— Geometry for integration of the infinitesimal interaction potential between two BAM halos of density (13) separated by z. Note symmetry about the azimuth.

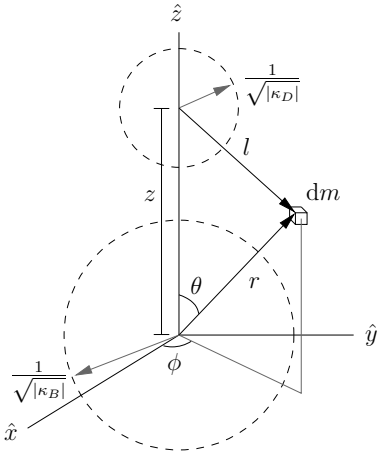

the halo, and

$$M_{\rm H}(z) = \frac{2^4\epsilon}{\sqrt{|\kappa_A|}} \tan^{-1}\left(\frac{z\sqrt{|\kappa_A|}}{2}\right) - \frac{2^5 z\epsilon}{|\kappa_A| z^2 + 4} \quad (24)$$

is the enclosed halo mass at distance z from this center. Explicitly we find

$$\Phi_{hb}(z) = -\frac{2^4 m_b \epsilon}{z\sqrt{|\kappa_A|}} \tan^{-1}\left(\frac{z\sqrt{|\kappa_A|}}{2}\right) \quad (25)$$

which is Newtonian for $z \gg 2/\sqrt{|\kappa_A|}$ and naturally softened for small separations

$$\lim_{z\to 0} \Phi_{hb}(z) = -8 m_b \epsilon. \quad (26)$$

3.2. *Halo-halo interaction*

To determine the interaction potential between two halos, we consider equation (25) with m_b replaced by an infinitesimal mass element of a separate halo with scale $|\kappa_D|$

$$\mathrm{d}m = \rho_h(l, \kappa_D) r^2 \sin\theta \mathrm{d}\theta \mathrm{d}r \mathrm{d}\phi. \quad (27)$$

Thus, BAM halo D is immersed in the potential of BAM halo A centered at a spherical coordinate origin (see Figure 2). From the law of cosines

$$l = \sqrt{r^2 + z^2 - 2zr\cos\theta} \quad (28)$$

and we thus find the following integral for the interaction potential

$$\Phi_{hh}(z) = -\frac{2^8\epsilon^2|\kappa_D|}{\pi\sqrt{|\kappa_A|}} \int \frac{r \tan^{-1}\left(r\sqrt{|\kappa_A|}/2\right)}{\left(|\kappa_D| l^2 + 4\right)^2} \, \mathrm{d}^3\mathbf{r}. \quad (29)$$

After integrations over the angular variables, proceeding with the following substitutions

$$u \equiv \frac{r\sqrt{|\kappa_A|}}{2} \qquad w^2 \equiv \frac{|\kappa_A|}{|\kappa_D|} \qquad q(z) \equiv \frac{z\sqrt{|\kappa_A|}}{2} \quad (30)$$

we find

$$\Phi_{hh}(z) = -\frac{z}{q} \int_0^\infty \frac{2^7 w^2 \epsilon^2 u \tan^{-1}(u) \, \mathrm{d}u}{\left[(u-q)^2 + w^2\right]\left[(u+q)^2 + w^2\right]}. \quad (31)$$

This integral is similar to those considered by Glasser (1968) and may be evaluated as follows: noting the integrand is even, consider $u \in (-\infty, \infty)$. After partial fractions over the real numbers, it can be seen that both summands evaluate to the same integral. Let $v \equiv u - q$. By translation invariance, the integral is unchanged and the parameter q now appears in the argument of the inverse tangent. After differentiation under the integral with respect to q, the resulting integral over v can be evaluated immediately by contour methods. The final integration over q gives

$$\Phi_{hh}(z) = \frac{-2^7\pi\epsilon^2}{z\sqrt{|\kappa_A\kappa_D|}} \cot^{-1}\left(\frac{\sqrt{|\kappa_A|} + \sqrt{|\kappa_D|}}{z\sqrt{|\kappa_A\kappa_D|}/2}\right). \quad (32)$$

Note that equation (32) is manifestly symmetric in κ_* as it must be by Newton's 3^{rd} law. The interaction potential (32) can be written more transparently with the aid of equation (14)

$$\Phi_{hh}(z) = -\frac{2M_D M_A}{\pi z} \cot^{-1}\left(\frac{\langle M\rangle}{2\pi\epsilon z}\right) \quad (33)$$

where M_A and M_D are the total enclosed masses of BAM halos A and D respectively, with $\langle M\rangle$ their arithmetic mean.

3.3. *Discussion*

To discuss interesting limiting cases, we consider only $\Phi_{hh}(z)$: the analysis for $\Phi_{hb}(z)$ proceeds identically with a change of constants. This is because $\tan^{-1}(x) = \cot^{-1}(1/x)$, and we see that expression (32) has the same functional form as expression (25). Inspection of expression (32) gives a length scale where the argument of $\cot^{-1}$ is order unity

$$z_{hh} \approx 4\langle r_0\rangle \quad (34)$$

which is just four times the average core radius of the two halos under consideration. Here we have used that $r_0 \equiv 1\sqrt{|\kappa|}$. For $z \gg z_{hh}$, we find that the interaction force

$$\mathbf{F}(z) = -\frac{M_D M_A}{z^2}\left[1 - \frac{\langle M\rangle}{z\pi^2\epsilon} + O\left(\frac{1}{z^3}\right)\right]\hat{\mathbf{z}} \quad (35)$$

is explicitly Newtonian with a leading dipole adjustment, which will act to diminish the force. At $z \ll z_{hh}$, the force law is dramatically altered

$$\mathbf{F}(z) = -\frac{2^8\pi^2\epsilon^3 z}{3\left[3\langle M\rangle + M_A^2/M_D + M_D^2/M_A\right]}\hat{\mathbf{z}} \quad (36)$$

consistent with a softening of the potential (33) at small separations

$$\lim_{z\to 0} \Phi_{hh}(z) = -4\epsilon\frac{M_D M_A}{\langle M\rangle}. \quad (37)$$

We note several useful properties of equation (35). Since the long-range interaction is Newtonian, on scales larger than typical core radii, one would expect gravitational formation of structure to be qualitatively unaltered. Thus an ensemble of cored halos will exhibit similar behaviour as (orders of magnitude more) cold dark matter particles within an N-body simulation on cosmological scales. On scales of galactic clusters, we expect qualitatively similar behaviour to that reported in

Clowe et al. (2006), but deviations from simulated behaviors (Springel & Farrar 2007) should become apparent. As the leading multipole correction enters as a dipole, these deviations from pure Newtonian predictions may be accessible at present observational uncertainties. Further, the next correction enters at the octupole, and so higher order terms need not be considered in a first treatment. The boundedness of the interaction potential (32) $\forall$ z removes the need to introduce an *ad hoc* softening procedure within N-body simulations. Since our predicted softening is physical, the spatial resolution of simulations involving BAM halos may be extended to well below kpc scales.

Though not immediately relevant for observation, the RW spacetimes' present day matter densities ρ_* must be large enough to ensure matter domination over their respective spatial curvatures κ_*. Constraint from Table 1 implies large ρ_*, but still many decades within matter-domination. To tune the time of a halo's zero density, one considers a radiation dominated ansatz instead of ansatz (9). This does not alter the asymptotic behaviour of the BAM halo and simply reflects the Copernican assumption that the associated RW spacetime should also have undergone a hot Big Bang. The time of halo zero density can then be adjusted to well within our own epoch of radiation domination, by freely adjusting the RW spacetime's present day matter to radiation ratio.

4. LIMITATIONS

While the simplest WIMP CDM scenarios can choose a single mass for all particles, the distribution of BAM spatial curvature κ is not presently constrained, only the integrated mass over all halos. The nature of this distribution is an open question. Furthermore, WIMP CDM scenarios can begin accretion after freeze-out, with nucleation around overdensities seeded by a primordial inflation driven by a field whose decay also created the WIMPs. We refrain from speculation on the origins of $N \approx 10^{12}$ distinct RW spacetimes.

The Jeans analysis employed to determine halo fit parameters from velocity dispersion measurements requires an assumed three dimensional distribution of luminous mass. While we have made the standard assumption of a Plummer distribution, other distributions in projection may agree with observed surface brightnesses. Work presently underway to remove luminous assumptions from the Jeans model will permit investigation into the robustness of the experimental results presented.

5. CONCLUSION

The unanticipated production of a dark, pseudo-isothermal density as a byproduct of a model independent, purely geometric, inflationary scenario has motivated our construction of a cored halo $\sim 1/r^4$. Our halo originates from the radial pressure term of a distinct Robertson-Walker spacetime's Ricci tensor, grows from zero density at some time in the past to a bounded value, and encloses finite mass over all space. These Boulanger Astrophysically Motivated (BAM) halos feature a novel reciprocal square scaling relation $\rho_0 \propto r_0^{-2}$ between central density ρ_0 and core radius r_0. We have confirmed this scaling relation with computed fits to published astrophysical data on the classical Milky Way dwarf spheroidal galaxies. Since the BAM halo encloses finite mass, interactions can be regarded as two-body pointlike through a force Newtonian at large separations which decreases to zero at small separations. We show that ensembles of very many BAM halos would behave in a qualitatively similar manner to cold dark matter on cosmological scales, thus potentially resolving tension between N-body simulations on large scales and astrophysical observations on galactic scales.

The author warmly acknowledges M. G. Walker for performing the fit computations and for extended correspondence during the preparation of this work. The author further thanks M. L. Glasser for his elegant integration procedure shared in private correspondence and T. Browder for frequent feedback.

APPENDIX

In this brief appendix, we explicitly derive the purely mathematical result (4). Introduce a flat metric (1) and a separate Robertson-Walker (RW) metric (2) on the same manifold. Consider the Ricci tensor of metric (2)

$$R_{rr} = \frac{2\kappa_A + a\ddot{a} + 2\dot{a}^2}{1 - \kappa_A r^2} \qquad R_{tt} = -\frac{3\ddot{a}}{a} \tag{A1}$$
$$R_{\theta\theta} = \frac{2\kappa_A + a\ddot{a} + 2\dot{a}^2}{r^{-2}} \qquad R_{\phi\phi} = \frac{2\kappa_A + a\ddot{a} + 2\dot{a}^2}{r^{-2}\sin^{-2}\theta}$$

and form the scalar quantity

$$R_{\mu\nu}\eta^{\mu\nu} = \frac{3\ddot{a}}{a} + \left(2\kappa_A + a\ddot{a} + 2\dot{a}^2\right)\left[\frac{1}{1 - \kappa_A r^2} + 2\right]. \tag{A2}$$

If we enforce the constraint (3) with $\kappa_A \neq 0$, we find

$$3\frac{\ddot{a}}{a} + 2a\ddot{a} + 4\dot{a}^2 + 4\kappa_A = 0. \tag{A3}$$

This is a non-linear, separable, ordinary differential equation in a for $\dot{a}$. Given $\kappa_A < 0$, the solution for initial conditions $a(0) = \dot{a}(0) = 0$ is found to be

$$\dot{a} = \sqrt{|\kappa_A|}\sqrt{1 - \frac{1}{\left(2a^2/3 + 1\right)^2}}. \tag{A4}$$

For $a \ll \sqrt{3/2}$ we can Taylor expand the radicand about 0. We find

$$\dot{a} = \sqrt{\frac{4|\kappa_A|}{3}} a \tag{A5}$$

implying exponential growth of the scale factor, establishing the inflationary claim. Substitution of equation (A4) into equation (A2) gives

$$R_{\mu\nu}\eta^{\mu\nu} = -\frac{54|\kappa_A|}{(3+2a^2)^3} \frac{1}{1+|\kappa_A| r^2}. \tag{A6}$$

which is the desired result (4).

REFERENCES

Ade, P. A. R. et al. 2013, ArXiv e-prints, 1303.5062
Ahn, C. P. et al. 2012, ApJS, 203, 21, 1207.7137
Begeman, K. G., Broeils, A. H., & Sanders, R. H. 1991, MNRAS, 249, 523
Bertone, G., Hooper, D., & Silk, J. 2005, Phys.Rept., 405, 279, hep-ph/0404175
Boulanger, N., Damour, T., Gualtieri, L., & Henneaux, M. 2001, Nuclear Physics B, 597, 127, hep-th/0007220
Burkert, A. 1995, ApJ, 447, L25, astro-ph/9504041
Clowe, D., Bradač, M., Gonzalez, A. H., Markevitch, M., Randall, S. W., Jones, C., & Zaritsky, D. 2006, ApJ, 648, L109, astro-ph/0608407
de Blok, W. J. G. 2010, Advances in Astronomy, 2010, 0910.3538
Donato, F. et al. 2009, MNRAS, 397, 1169, 0904.4054
Glasser, M. 1968, Mathematics of Computation, 445
Hinshaw, G. et al. 2013, ApJS, 208, 19, 1212.5226
Mateo, M. L. 1998, ARA&A, 36, 435, astro-ph/9810070
Navarro, J. F., Frenk, C. S., & White, S. D. M. 1997, ApJ, 490, 493, astro-ph/9611107
Salucci, P., Wilkinson, M. I., Walker, M. G., Gilmore, G. F., Grebel, E. K., Koch, A., Frigerio Martins, C., & Wyse, R. F. G. 2012, MNRAS, 420, 2034, 1111.1165
Springel, V., & Farrar, G. R. 2007, MNRAS, 380, 911, astro-ph/0703232
Springel, V. et al. 2005, Nature, 435, 629, astro-ph/0504097
Walker, M. G., Mateo, M., Olszewski, E. W., Peñarrubia, J., Wyn Evans, N., & Gilmore, G. 2009, ApJ, 704, 1274, 0906.0341
——. 2010, ApJ, 710, 886
Walker, M. G., & Peñarrubia, J. 2011, ApJ, 742, 20, 1108.2404
Zavala, J., Vogelsberger, M., & Walker, M. G. 2013, MNRAS, 431, L20, 1211.6426
Zwicky, F. 1937, ApJ, 86, 217